Analysis of the Stability and Accuracy of Numerical Methods Applied to the Simulation of Electromagnetic Transients Involving Double Integration Steps.

R. L. Silva, F. A. Moreira, A. C. S. de Lima

***Abstract*--This paper presents an analysis of some numerical integration methods that can be used for multirate simulation in electromagnetic transient programs. Among the existing methods, the trapezoidal, backward Euler and Simpson's integration rules will be evaluated. These methods are analyzed regarding characteristics such as accuracy and stability when applied to the simulation of electrical transients involving two different time steps. The transient solution of an RLC network is then presented using these numerical methods and simulating it with double integration time steps.**

***Keywords*: Numerical integration methods, Multirate simulation, Accuracy of integration rules, Stability of integration rules.**

I. Introduction

THE time domain simulation plays a key role in the design and analysis of electrical networks. The EMTP (Electromagnetic Transients Program) [1], in its several versions, is regarded as the leading tool for the simulation of electromagnetic transients in power systems. However, this tool has a limitation that is the necessity of using a single integration step for the entire network. As a result, the size of this step is determined by the characteristics of the elements that have faster dynamics, possibly resulting in a waste of computational resources, since the integration step could be larger for certain network components with slower dynamics.

This context has led several groups of researchers to seek new techniques capable of performing faster simulations without sacrificing accuracy and stability. In the 1980's and 1990's, the possibility of using two or more different time steps for simulation of electrical networks was the focus of several studies, both for the simulation of electronic circuits and for the simulation of power systems [2]-[3]. There are also recent works that continue exploring this possibility [4]-[5]. This paper presents an analysis of accuracy and stability of some integration rules used for the simulation of electromagnetic transients when applying the technique developed in [6] for the simulation of power systems with multiple time steps, also called latency exploitation

The remainder of this paper is organized as follows. Section II summarizes the technique adopted for the simulation with double time steps, although it may be extended to multiple time steps as well. Section III presents the modifications performed in some integration rules for double time step simulations. In sections IV and V, the stability and accuracy of the integration rules for the double time step scenario are analyzed, respectively. In section VI, some simulation results are presented. Finally, in section VII, the conclusions are stated.

II. Simulation method with double integration steps

The method used in this work for the time-domain simulation of a network with more than one integration step, is applied in the context of a partitioned network which is divided into subnetworks connected by links [7]. The partitioning technique is based on the recognition that some subsystems may have large time constants, and therefore can be simulated with large time steps, and other subsystems may have small time constants, requiring consequently smaller time steps [6]. Fig. 1 shows a network partitioned into fast and slow subsystems, connected through a link. Each subsystem contains any combination of voltage and current sources, passive elements, and transmission lines. They are connected through a resistance in this case, although any other element could have been chosen as a link.

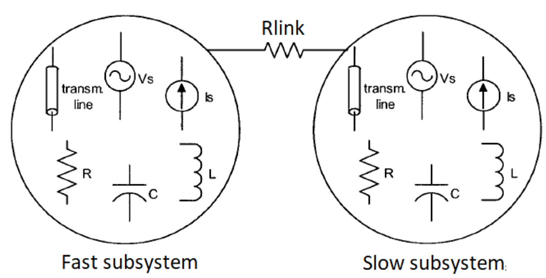

Fig. 1. Diagram of a generic network partitioned into a fast subsystem and a slow one.

The MATE (Multi-Area Thévenin Equivalent) concept [7] guarantees an accurate solution of the complete network for a single time step solution if both subsystems are first solved

This work was supported in part by CNPq.

R. L. Silva is with SENAI, Salvador, BA, Brazil (e-mail: eng.ricardogalvao@yahoo.com.br).

F. A. Moreira is with the Department of Electrical Engineering, Federal University of Bahia, Salvador, BA, Brazil (e-mail: moreiraf@ufba..br).

A. C. S. de Lima is with the Department of Electrical Engineering, Federal University of Rio de Janeiro, RJ, Brazil (e-mal: acsl@dee.ufrj.edu.br).

Paper submitted to the International Conference on Power Systems Transients (IPST2019) in Perpignan, France June 17-20, 2019.

separately, as if they were completely decoupled and then the nodal voltages are recalculated taking into account the current flowing through the link. Even if different integration steps are used, it is still possible to ensure accurate results if each of the subsystems can be well characterized as being either slow or fast.

In the technique already presented in previous contributions [6, 8] the time step set for the slow subsystem must always be an integer multiple of the fast subnetwork time step. By setting ΔT as the large time step and Δt as the small time step, this relationship can be expressed as

$$\Delta T = n\Delta t \tag{1}$$

where $n > 1$. In this work, the analysis will be performed with only two time steps, although a greater number of time steps can be used following the framework presented.

Fig. 2 shows a timeline of a general network simulation when a double time step simulation is performed.

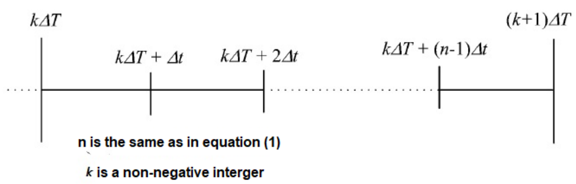

Fig. 2. Simulation timeline with two distinct time steps.

For a synchronized solution, both subsystems are solved together at instants multiple of ΔT. The particularity of the method is that for the time steps located between two consecutive ΔT's intervals, only the fast subsystem is solved.

III. Integration Rules for Simulation with Double-Time Step.

To verify the efficiency of the method proposed, this study will analyze the behavior of three numerical integration rules for the discretization of the differential equations relating voltage and current in inductors and capacitors when working with two different time steps. From the equations in the continuous time domain:

$$i_c(t) = \mathrm{C}\frac{dv_c(t)}{dt} \tag{2}$$

$$\mathrm{v}_L(t) = \mathrm{L}\frac{di_L(t)}{dt} \tag{3}$$

where $v_c(t)$, $v_L(t)$, $i_c(t)$, and $i_L(t)$ are the voltage in a capacitor, the voltage in an inductor, the current in a capacitor and the current in an inductor, respectively.

A. Trapezoidal rule

Integrating both sides of (2) and (3) from $t-\Delta T$ to t leads to

$$\int_{t-\Delta T}^{t} v_L(t)dt = L[(i_L(t) - i_L(t-\Delta T)] \tag{4}$$

$$\int_{t-\Delta T}^{t} i_c(t)dt = C[(v_c(t) - v_c(t-\Delta T)] \tag{5}$$

Applying the trapezoidal integration rule to (4) and (5), and considering all solutions between two consecutive large steps, results in

$$\int_{t-\Delta T}^{t} v_L(t)dt = \frac{\Delta t}{2}[(v_L(t) + v_L(t-\Delta T)] + \Delta t\sum_{k=1}^{n-1} v_L(t-\Delta \mathrm{T} + k\Delta \mathrm{t}) \tag{6}$$

$$\int_{t-\Delta T}^{t} i_c(t)dt = \frac{\Delta t}{2}[(i_c(t) + i_c(t-\Delta T)] + \Delta t\sum_{k=1}^{n-1} i_c(t-\Delta \mathrm{T} + k\Delta \mathrm{t}) \tag{7}$$

The equations relating voltage and current in an inductor and a capacitor in discrete time can be written as:

$$i_L(t) = \frac{\Delta t}{2L}v_L(t) + h_L(t) \tag{8}$$

$$i_c(t) = \frac{2C}{\Delta t}v_c(t) + h_c(t) \tag{9}$$

The history terms are given by:

$$h_L(t) = i_L(t-\Delta T) + \frac{\Delta t}{2L}v_L(t-\Delta T) + \frac{\Delta t}{L}\sum_{k=1}^{n-1} v_L(t-\Delta T + k\Delta t) \tag{10}$$

$$h_c(t) = -\frac{2C}{\Delta t}v_c(t-\Delta T) - i_c(t-\Delta T) - 2\sum_{k=1}^{n-1} i_c(t-\Delta T + k\Delta t) \tag{11}$$

Equations (10) and (11) generate the history sources for an inductor and a capacitor, respectively, with all the information gathered from these elements within the large integration step ΔT.

This avoids the almost randomness of just considering the individual values of the last calculated solution from the fastest subnetwork. The number of numerical operations does not increase significantly when the history terms of the fast elements have to be finally updated so that the complete network may be solved together, since they are continuously accumulated at each small Δt [8].

B. Backward Euler rule

Applying the backward Euler rule for (2) and (3), voltage and current ratios of an inductor and a capacitor in the discretized time domain can be obtained leading to, after some mathematical manipulations:

$$\int_{t-\Delta T}^{t} v_L(t)dt = \Delta t v_L(t) + \Delta t\sum_{k=1}^{n-1} v_L(t-\Delta T + k\Delta t) \tag{12}$$

$$\int_{t-\Delta T}^{t} i_c(t)dt = \Delta t i_c(t) + \Delta t\sum_{k=1}^{n-1} i_c(t-\Delta T + k\Delta t) \tag{13}$$

In compact form the following equations may be derived for the backward Euler rule:

$$i_L(t) = \frac{\Delta t}{L}v_L(t) + h_L(t) \tag{14}$$

$$i_c(t) = \frac{C}{\Delta t}v_c(t) + h_c(t) \tag{15}$$

The history terms, considering all the information gathered for the larger integration step ΔT are given by

$$h_L(t) = i_L(t - \Delta T) + \frac{\Delta t}{L}\sum_{k=1}^{n-1} v_L(t - \Delta T + k\Delta t) \quad (16)$$

$$h_c(t) = -\frac{C}{\Delta t} v_L(t - \Delta T) - \sum_{k=1}^{n-1} i_c(t - \Delta T + k\Delta t) \quad (17)$$

C. Simpson's rule

The Simpson rule consists in the hypothesis of approximating the derivative of a function to be integrated by a second-degree function.

Applying the same development as before to (2) and (3), the following equations may be derived:

$$i_L(t) = \frac{\Delta t}{3L} v_L(t) + h_L(t) \quad (18)$$

$$i_c(t) = \frac{3C}{\Delta t} v_c(t) - h_c(t) \quad (19)$$

The history terms are given by

$$h_L(t) = i_L(t - 2\Delta T) + \frac{\Delta t}{3L}[4v_L(t - \Delta T) + v_L(t - 2\Delta T)] + \left(\frac{\Delta t}{L}\sum_{k=1}^{n-1} v_L(t - 2\Delta T + k\Delta t)\right) \quad (20)$$

$$h_c(t) = -\frac{3C}{\Delta T} v_c(t - 2\Delta T) - 4i_c(t - \Delta T) - i_c(t - 2\Delta T) - 3\sum_{k=1}^{n-1} i_c(t - 2\Delta T + k\Delta t) \quad (21)$$

IV. Analysis of the Stability of the Integration Rules for Simulation with Double-Time Step

In this section, the stability of the integration rules presented in the previous section will be analyzed for the case of double time steps. The z-transform is applied to the difference equations and the poles and zeros shall be checked.

A. Trapezoidal rule

Applying for an inductor an entry in the form $v_L(t) = e^{j\omega t}$ and assuming the output in the form $i_L(t) = Ye(\omega)e^{j\omega t}$ to (8), where $Y_e(\omega)$ is the admittance in the frequency domain, in terms of the small time step *Δt*, after some manipulation it is possible to obtain:

$$Ye(\omega) = \frac{\Delta t}{2L}\left[\frac{e^{j\omega n\Delta t} + 1}{e^{j\omega n\Delta t} - 1}\right] + \frac{\Delta t}{2L}\left[\frac{2\sum_{k=1}^{n-1} e^{j\omega k\Delta t}}{e^{j\omega n\Delta t} - 1}\right] \quad (22)$$

Replacing $e^{j\omega\Delta t}$ by *z*, the transfer function in the z-domain is then given by

$$Ye(\omega) = \frac{\Delta t}{2L}\left[\frac{z^n + 1 + 2\sum_{k=1}^{n-1} z^k}{z^n - 1}\right] \quad (23)$$

Expanding (23) results in

$$Ye(\omega) = \frac{\Delta t}{2L}\left[\frac{(z+1)}{(z-1)}\frac{(z+z_2)}{(z+z_2)}\cdots\frac{(z+z_n)}{(z+z_n)}\right] = \frac{\Delta t}{2L}\left[\frac{z+1}{z-1}\right] \quad (24)$$

Equation (24) is the same transfer function obtained for the trapezoidal rule for the single time step case as it can be verified in [9]. It is possible to notice that the transfer function has a pole in z = 1 and a zero in z = −1, and the system is stable for both the integrator and the differentiator. However, the pole in z = −1 for the equivalent differentiator introduces numerical bounded oscillations at discontinuities, as when a single time step is used.

B. Backward Euler rule

Applying an entry in the form $v_L(t) = e^{j\omega t}$ and assuming the output in the form $i_L(t) = Ye(\omega)e^{j\omega t}$ to (14), where $Ye(\omega)$ is the admittance in the frequency domain, in terms of the small time step *Δt*, after some manipulation it is possible to obtain

$$Ye(\omega) = \frac{\Delta t}{L}\left[\frac{e^{j\omega n\Delta t}}{e^{j\omega n\Delta t} - 1}\right] + \frac{\Delta t}{L}\left[\frac{\sum_{k=1}^{n-1} e^{j\omega k\Delta t}}{e^{j\omega n\Delta t} - 1}\right] \quad (25)$$

Replacing $e^{j\omega\Delta t}$ by *z*, the transfer function is then given by

$$Ye(\omega) = \frac{\Delta t}{L}\left[\frac{z^n + \sum_{k=1}^{n-1} z^k}{z^n - 1}\right] \quad (26)$$

Expanding (26) results in

$$Ye(\omega) = \frac{\Delta t}{L}\left[\frac{z}{(z-1)}\frac{(z+z_2)}{(z+z_2)}\cdots\frac{(z+z_n)}{(z+z_n)}\right] = \frac{\Delta t}{L}\left[\frac{z}{z-1}\right] \quad (27)$$

The transfer function has a pole in z = 1 and a zero in z = 0, exactly the same as when the single integration step is used [9], and the system is again stable for both the integrator and differentiator. The pole in z = 0 for the equivalent differentiator makes the system critically damped as a differentiator, as already occurs in the case of a single integration step [10].

C. Simpson's rule

It is again assumed an entry in the form $v_L(t) = e^{j\omega t}$ and assuming the output in the form $i_L(t) = Ye(\omega)e^{j\omega t}$ in (18), the admittance in the frequency domain for the Simpson rule is given by:

$$Ye(\omega) = \frac{\Delta t}{3L}\left[\frac{e^{j\omega 2n\Delta t} + 4e^{j\omega n\Delta t} + 1}{e^{j\omega 2n\Delta t} - 1}\right] + \frac{\Delta t}{3L}\left[\frac{3\sum_{k=1}^{n-1} e^{j\omega k\Delta t}}{e^{j\omega 2n\Delta t} - 1}\right] \quad (28)$$

Replacing $e^{j\omega\Delta t}$ by *z*, the transfer function is then given by

$$Ye(\omega) = \frac{\Delta t}{3L}\left[\frac{z^{2n} + 4z^n + 1}{z^{2n} - 1}\right] + \frac{\Delta t}{3L}\left[\frac{3\sum_{k=1}^{n-1} z^k}{z^{2n} - 1}\right] \quad (29)$$

Expanding (29), results in

$$Ye(\omega) = \frac{\Delta t}{3L}\left[\frac{z^2 + 4z + 1}{z^2 - 1}\frac{(z+z_2)}{(z+z_2)}\cdots\frac{(z+z_n)}{(z+z_n)}\right] = \frac{\Delta t}{3L}\left[\frac{z^2 + 4z + 1}{z^2 - 1}\right] \quad (30)$$

The transfer function has poles in z = ±1 and zeros in z = −0.268 and z = −3.732. Therefore the Simpson rule is stable as an integrator, although it may become unstable as a differentiator.

V. Analysis of the Accuracy of the Integration Rules for Simulation with Double-Time Step

A. Trapezoidal rule

For accuracy analysis, (22) can be rewritten as

$$Ye(\omega) = Ye^{(1)}(\omega) + Ye^{(2)}(\omega) \tag{31}$$

where

$$Ye^{(1)}(\omega) = \frac{\Delta t}{2L}\left[\frac{e^{j\omega n\Delta t}+1}{e^{j\omega n\Delta t}-1}\right] \tag{32}$$

$$Ye^{(2)}(\omega) = \frac{\Delta t}{2L}\left[\frac{2\sum_{k=1}^{n-1} e^{j\omega k\Delta t}}{e^{j\omega n\Delta t}-1}\right] \tag{33}$$

Both the terms $Ye^{(1)}(\omega)$ and $Ye^{(2)}(\omega)$ depend on the ratio between the integration steps $n = \Delta T/\Delta t$. However, the number of terms in $Ye^{(2)}(\omega)$ increases as $\boldsymbol{n}$ grows. The equivalent inductance $Le^{(1)}(\omega)$, after some manipulation, can be obtained from (32) as

$$Le^{(1)}(\omega) = nL\frac{tan(\frac{\omega n\Delta t}{2})}{\frac{\omega n\Delta t}{2}} \tag{34}$$

The frequency-dependent distortion factor $ke^{(1)}(\omega)$ can then be obtained:

$$Ke^{(1)}(\omega) = n\frac{tan(\frac{\omega n\Delta t}{2})}{\frac{\omega n\Delta t}{2}} \tag{35}$$

It is possible to verify that the distortion factor $ke^{(1)}(\omega)$ is $\boldsymbol{n}$ times greater than the distortion of the trapezoidal rule with a single time step. From (33), one can write $Ye^{(2)}(\omega)$ as

$$Ye^{(2)}(\omega) = \frac{\Delta t}{2L}\frac{\sum_{k=1}^{n-1}\cos[\omega\left(k-\frac{n}{2}\right)\Delta t]}{jsin(\frac{\omega n\Delta t}{2})} \tag{36}$$

With the equivalent inductance $Le^{(2)}(\omega)$ given by:

$$Le^{(2)}(\omega) = nL\frac{sin(\frac{\omega n\Delta t}{2})}{(\frac{\omega n\Delta t}{2})\sum_{k=1}^{n-1} cos[\omega(k-\frac{n}{2})\Delta t]} \tag{37}$$

The distortion factor $Ke^{(2)}(\omega)$ can then be obtained as

$$Ke^{(2)}(\omega) = n\frac{sin(\frac{\omega n\Delta t}{2})}{(\frac{\omega n\Delta t}{2})\sum_{k=1}^{n-1} cos[\omega(k-\frac{n}{2})\Delta t]} \tag{38}$$

The summation term present in the denominator of (38) takes into account all the contributions of the small time step solutions within the large time step ΔT.

The frequency response of the equivalent admittance $Ye(\omega)$ for the trapezoidal rule using double time step may be compared to the exact continuous time admittance $Y(\omega)$:

$$\frac{Ye(\omega)}{Y(\omega)} = \frac{1}{j\omega Le(\omega)}\Big/\frac{1}{j\omega L} = \frac{Ke^{(1)}(\omega)+Ke^{(2)}(\omega)}{Ke^{(1)}(\omega)Ke^{(2)}(\omega)} = \frac{1}{Ke(\omega)} \tag{39}$$

where $Ke(\omega)$ is the global distortion factor for the trapezoidal rule with two different time steps.

Fig. 3 shows the frequency response in magnitude and phase, given in per unit of the Nyquist frequency, for a particular situation where $\Delta T = 2\Delta t$.

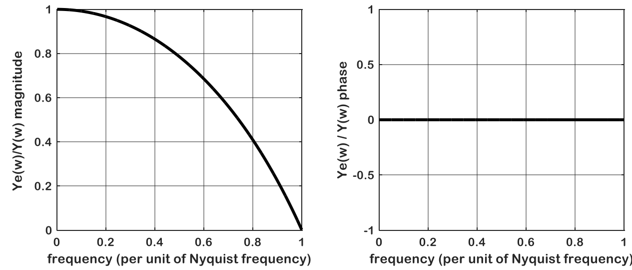

Fig. 3. Frequency response in magnitude and phase of the trapezoidal rule considering $\Delta T = 2\Delta t$.

If the frequency response shown in Fig. 3 is compared to the frequency response for the conventional single step trapezoidal integration rule or when considering larger ratios between ΔT and Δt, it is possible to verify that the history source accumulation procedure has not introduced any difference to the frequency response. This fact is detailed in [9]. It is concluded, therefore, that the accuracy of the simulation is not compromised for the fast part of the network as long as the large time step ΔT is adequate to represent the slower characteristic frequencies of the network.

B. Backward Euler rule

Rewriting (25) to better analyze the accuracy of the backward Euler integration rule for double time step simulation:

$$Ye^{(1)}(\omega) = \frac{\Delta t}{L}\left[\frac{e^{j\omega n\Delta t}}{e^{j\omega n\Delta t}-1}\right] \tag{40}$$

$$Ye^{(2)}(\omega) = \frac{\Delta t}{L}\left[\frac{\sum_{k=1}^{n-1} e^{j\omega k\Delta t}}{e^{j\omega n\Delta t}-1}\right] \tag{41}$$

Performing some manipulations in (40), results in

$$Ye^{(1)}(\omega) = \frac{\Delta t}{2L} + \frac{\Delta t}{2L}\left[\frac{1}{jtan(\frac{\omega n\Delta t}{2})}\right] \tag{42}$$

From (42) it is possible to visualize that there is a real part in the equivalent admittance in the case of the backward Euler rule. This real part corresponds to an equivalent conductance which is responsible for a phase distortion and the damping capabilities of the backward Euler rule [10].

The distortion factor $Ke^{(1)}(\omega)$ can be obtained after the appropriate algebraic manipulations, resulting in

$$Ke^{(1)}(\omega) = n\frac{tan(\frac{\omega n\Delta t}{2})}{\frac{\omega n\Delta t}{2}} \tag{43}$$

By executing the same procedures for $Ye^{(2)}(\omega)$, the distortion factor $Ke^{(2)}(\omega)$ can be obtained as

$$Ke^{(2)}(\omega) = n\frac{sin(\frac{\omega n\Delta t}{2})}{(\frac{\omega n\Delta t}{2})\sum_{k=1}^{n-1} cos[\omega(k-\frac{n}{2})\Delta t]} \tag{44}$$

The accuracy of the backward Euler rule can then be evaluated by comparing the frequency response of the equivalent admittance $Ye(\omega)$ to the exact continuous time admittance $Y(\omega)$.

The frequency response of the equivalent admittance $Ye(\omega)$

for the backward Euler rule using the double time step simulation may be compared to the exact continuous time admittance $Y(\omega)$.

$$\frac{Ye(\omega)}{Y(\omega)} = \left(\frac{\Delta t}{2L} + \frac{1}{j\omega Le(\omega)}\right)\Big/\frac{1}{j\omega L} = \frac{\mathrm{j}\Delta t\omega}{2} + \frac{Ke^{(1)}(\omega) + Ke^{(2)}(\omega)}{Ke^{(1)}(\omega)Ke^{(2)}(\omega)}$$

Fig. 4 shows the frequency response in amplitude and phase, given in per unit of the Nyquist frequency, assuming, once again, $\Delta T = 2\Delta t$:

Once again, when comparing to the single step backward Euler rule, no difference has been introduced when the history source accumulation procedure is adopted for the simulation with two different integration steps, therefore not compromising the accuracy of the simulation, at least for the fast part of the network [9].

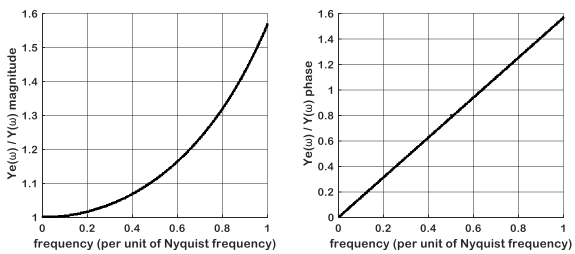

Fig. 4. Frequency response of the magnitude and phase of the backward Euler for the case of $\Delta T = 2\Delta t$.

C. Simpson's rule

From (28) one can write:

$$Ye(\omega) = Ye^{(1)}(\omega) + Ye^{(2)}(\omega) + Ye^{(3)}(\omega) \tag{45}$$

Applying the same procedure previously performed for the Euler and trapezoidal rules, the distortion factor associate to each equivalent admittance can be determined by

$$Ke^{(1)}(\omega) = \frac{n}{3}\frac{tan(\frac{\omega n\Delta t}{2})}{\frac{\omega n\Delta t}{2}} \tag{46}$$

$$Ke^{(2)}(\omega) = \frac{n}{3}\frac{sen(\frac{\omega\Delta T}{2})}{(\frac{\omega\Delta T}{2})\sum_{k=1}^{n-1} cos[\omega(k-\frac{n}{2})\frac{\Delta T}{n}]} \tag{47}$$

$$Ke^{(3)}(\omega) = \frac{2n}{3}\frac{sen(\frac{\omega\Delta T}{2})}{(\frac{\omega\Delta T}{2})\sum_{k=1}^{n-1} cos[\omega(k-\frac{n}{2})\frac{\Delta T}{n}]} \tag{48}$$

Fig. 5 shows the frequency response in amplitude and phase, assuming again, $\Delta T = 2\Delta t$.

The Simpson's rule is accurate for frequencies below 0.4 pu of the Nyquist frequency. It is interesting to notice that it has a distinct behavior in magnitude and phase below and above half the Nyquist frequency.

VI. Simulation Results

An example proposed in [8] was chosen for the purpose of presenting simulation results using two different time steps for the three integration rules discussed in this manuscript.

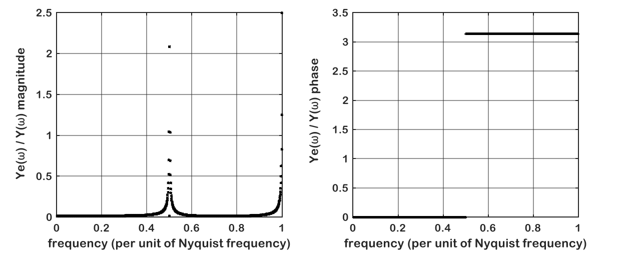

Fig. 5. Frequency response in magnitude and phase of the Simpson's rule for the case $\Delta T = 2\Delta t$.

Fig. 6 shows the proposed circuit where V_{fast} is the fast capacitor (1μF) voltage and V_{slow} is the slow capacitor (100μF) voltage. This is a simple circuit where the dominant eigenvalues in each of the subnetworks are reasonably independent [11]. Therefore, it is ideal for the double time step simulation. The voltage source, with a frequency of 60 Hz and an amplitude of 1.0 V has been connected for a long time, and the switch closes at t = 0. Three different simulation methods are chosen and tested using the integration rules previously analyzed, as follows:

1. Simulation using the shortest time step to ensure maximum accuracy for the complete network: Δt = 0.2 μs;
2. Two different time steps: Δt = 0.2 μs for the fast part of the network and ΔT = 2.0 μs for the slow part;
3. Simulation using the large time step for the complete network: ΔT = 2.0 μs.

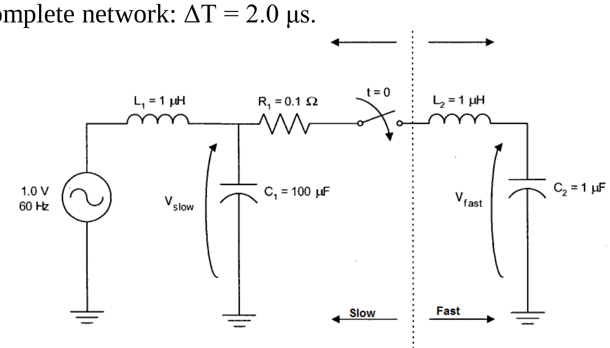

Fig. 6. Network considered for the double time step simulation.

Fig. 7 shows the voltage across the capacitor of the fast part of the network for the three methods proposed when using the trapezoidal rule.

Fig. 8 shows the voltage across the fast capacitor for the three methods proposed when using the backward Euler integration rule.

Fig. 9 shows the voltage across the fast capacitor of the network for the three methods proposed when using the Simpson's rule.

By analyzing Fig. 7, it is possible to verify that the trapezoidal rule represents accurately the voltage across the fast capacitor when using the double time step method, as expected from the accuracy analysis presented in section V-A. The voltage across the fast capacitor, however, is not well represented when using the single large time step.

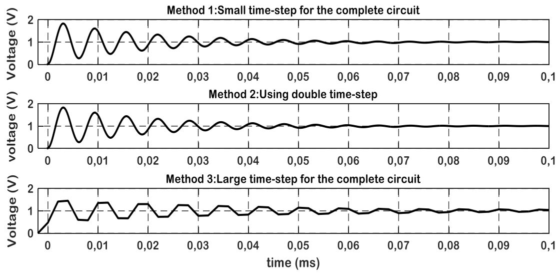

Fig. 7. Voltage across the capacitor C_2 ("fast") using trapezoidal rule.

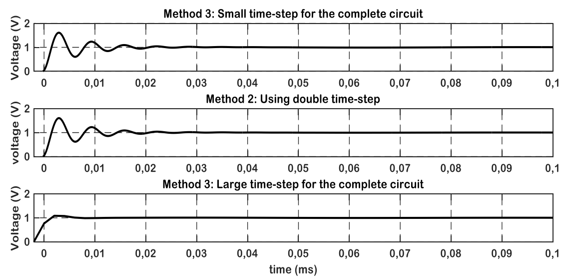

Fig. 8. Voltage across the capacitor C_2 ("fast") using backward Euler rule.

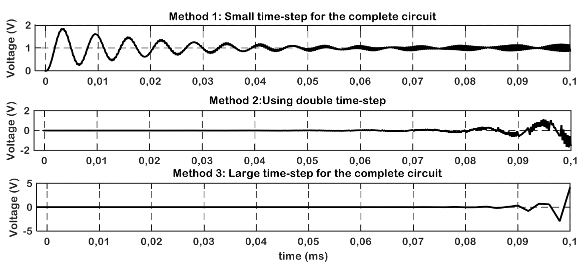

Fig. 9. Voltage across the capacitor C_2 ("fast") using Simpson's rule.

In the case of the backward Euler method (Fig. 9), the voltage in the fast capacitor when simulated with the double time step method has a good agreement with the single fast time step, as also expected from the accuracy analysis presented in section V-B. However, in both cases, there is an increased attenuation due to the equivalent conductance shown in (42). On the other hand, the Simpson's rule has demonstrated to be unstable for all the three methods. In particular, when using a small time-step for the complete circuit, the Simpson's rule gives accurate results for the initial voltage oscillations across the fast capacitor. However as the simulation time approaches 0.1 ms, growing oscillations start to appear which will eventually lead to numerical instability.

Fig. 10 shows the comparison of the three integration rules proposed in this work specifically for the case of double time step simulation: 0.2 μs for the fast part and 2.0 μs for the slow part. The voltage in the "fast" capacitor is shown.

The trapezoidal and backward Euler integration rules gave good results when using the double time step simulation method, although there is a considerable attenuation in the case of the backward Euler rule as previously mentioned. The Simpson's rule was unstable as expected from the stability analysis performed in section IV-C.

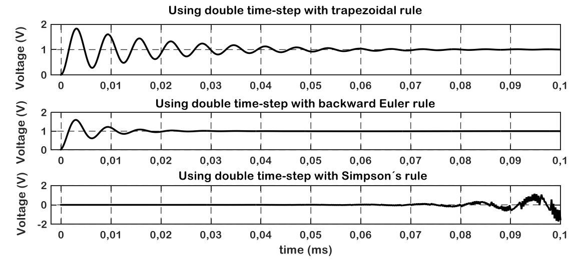

Fig. 10. Voltage across the capacitor C_2 ("fast"). For the three integration rules and considering the double time step simulation.

VII. CONCLUSIONS

In this work an analysis of some of the numerical integration rules that can be used for time-domain transients simulation has been performed when considering the possibility of executing the simulation with different integration steps in order to take advantage of the different time constants that distinct parts of a network may exhibit. The integration rules analyzed were trapezoidal, backward Euler, and Simpson's, and they have been evaluated both in terms of the accuracy and stability of the simulation. It was not the purpose of this work to demonstrate the decrease in the simulation time. A quantitative comparison is shown in [8].

The accuracy and stability of the trapezoidal and backward Euler rules under the double time step condition did not change when compared to the respective integration rules for a single time step for the fast capacitor. Due to the numerical damping, the backward Euler rule provides a greater attenuation of the electrical variables. The Simpson's rule did not present a satisfactory response due to its unstable behavior.

VIII. REFERENCES

[1] H. W. Dommel, "Digital computer solution of eletromagnectic transients in single and multiphase networks," *IEEE Trans. Power App. Syst*., vol. 88, pp. 388–399, 1969.

[2] R. A. Saleh and A. R. Newton,"The exploitation of double time-step and multirate behavior using nonlinear relaxation for circuit simulation," *IEEE Trans. CAD of Integ. Circ. and Syst*. vol. 8, no. 12, pp. 1286-1298, 1988.

[3] M. Crow and M. Ilic, "The parallel implementation of the waveform relaxation method for transient stability simulation," *IEEE Trans. Power Syst.*, vol. 5, pp. 922–932, 1990.

[4] F. Câmara, A. C. S. Lima, and F. A. Moreira, "A full frequency dependent line model based on folded line equivalencing and latency exploitation," *Elect. Power Syst. Res*., vol. 154, pp. 352–360, 2018.

[5] Q. Mu et al., "A multirate EMT co-simulation of large AC and MMC-based MTDC systems," IEEE Trans. Power Syst., vol. 33, pp. 1252-1263, 2018.

[6] F. A. Moreira, J. R Martí, L. C. Zanetta, and L. R. Linares, "Multirate simulations with simultaneous-solution using direct integration methods in a partitioned network environment," *IEEE Trans. Circ. and Syst. I: Reg. Papers*, vol. 53, no. 12, pp. 2765-2778, 2006.

[7] J. R. Martí, L. R. Linares, J. A. Hollman, and F. A. Moreira "OVNI: Integrated software/hardware solution for real-time simulation of large power systems," Proc. of the PSCC, Seville, Spain, 2002.

[8] F. A. Moreira and J. R. Martí, "Latency techniques for time-domain power system transients simulation," *IEEE Trans. Power Syst.*; vol. 20, pp. 246-253, 2005.

[9] F. A. Moreira, "Latency techniques for power system transients simulation," Ph.D. dissertation, Dept. Elect. Engin. Univ. British Columbia, Vancouver, 2002.

[10] J. Lin and J. R. Martí, "Implementation of the CDA procedure in the EMTP," *IEEE Trans. on Power Syst.*, vol. 5, pp. 394–402, 1990.

[11] F. A. Moreira and J. R. Martí, "Latency suitability for the time-domain simulation of electromagnetic transients through network eigenanalysis," Proc. of the IPST, New Orleans, USA, 2003.